DOI: 10.1002/JLB.1TA1117-431RR

JLB JOURNAL OF LEUKOCYTE BIOLOGY

TECHNICAL ADVANCE

Neutrophil progenitor populations of rhesus macaques

Kim L. Weisgrau[1] | **Logan J. Vosler**[1] | **Nicholas L. Pomplun**[1] | **Jennifer M. Hayes**[2] | **Heather A. Simmons**[2] | **Kristen R. Friedrichs**[3] | **Eva G. Rakasz**[1]

[1]Immunology Services Unit, Wisconsin National Primate Research Center, University of Wisconsin-Madison, Madison, Wisconsin, USA

[2]Clinical Pathology Unit, Wisconsin National Primate Research Center, University of Wisconsin-Madison, Madison, Wisconsin, USA

[3]Pathobiological Sciences, School of Veterinary Medicine, University of Wisconsin-Madison, Madison, Wisconsin, USA

Correspondence
Eva G. Rakasz, Ph.D., AIDS Vaccine Research Laboratory, 585 Science Drive, Madison, WI 53711, USA.
Email: erakasz@primate.wisc.edu

Abstract

Captive-bred rhesus macaques of Indian origin represent one of the most important large animal models for infectious disease, solid organ transplantation, and stem cell research. There is a dearth of information defining hematopoietic development, including neutrophil leukocyte differentiation in this species using multicolor flow cytometry. In the current study, we sought to identify cell surface markers that delineate neutrophil progenitor populations with characteristic immunophenotypes. We defined four different postmitotic populations based on their CD11b and CD87 expression pattern, and further refined their immunophenotypes using CD32, CD64, lactoferrin, and myeloperoxidase as antigenic markers. The four subsets contained myelocyte, metamyelocyte, band, and segmented neutrophil populations. We compared our flow cytometry-based classification with the classical nuclear morphology-based classification. We found overlap of immunological phenotype between populations of different nuclear morphology and identified phenotypically different subsets within populations of similar nuclear morphology. We assessed the responsiveness of these populations to stimulatory signals, such as LPS, fMLP, or PMA, and demonstrated significant differences between human and rhesus macaque neutrophil progenitors. In this study, we provided evidence for species-specific features of granulopoiesis that ultimately manifested in the divergent immunophenotypes of the fully differentiated segmented neutrophils of humans and rhesus macaques. Additionally, we found functional markers that can be used to accurately quantify neutrophil progenitors by flow cytometry. Although these markers do not coincide with the classical nuclear-morphology-based grading, they enable us to perform functional studies monitoring immunophenotypic markers.

KEYWORDS

bone marrow, immunophenotype, neutrophil progenitors, rhesus macaque

1 | INTRODUCTION

Neutrophil leukocytes are the most abundant WBCs in circulation. They represent first responders in any type of injury or inflammation.[1,2] Mature neutrophils are nondividing cells with a lifespan of several days.[3,4] Therefore, their homeostasis requires continuous replenishment supported by an uninterrupted differentiation process in the bone marrow. Differentiation stages of human neutrophil progenitor cell populations are distinguished according to their nuclear morphology. In successive order, these are myeloblasts, promyelocytes, myelocytes, metamyelocytes, bands, and segmented neutrophils.[5] Accurate quantitation of these cell populations with Wright–Giemsa staining and microscopy is time consuming, inefficient, lacks any information about their functional capabilities, phenotypic heterogeneity, and provides no insights regarding through what steps neutrophil differentiation happens.[6] Quantitation using flow cytometry-based methods might offer significant improvement provided that appropriate differentiation markers are identified.[7,8] In the case of human neutrophil progenitors, these critical differentiating markers have been the CD11b (complement receptor [CR] 3), CD15 (Lewis-x), CD16 (FcRγ III), CD33, and the CD49d (VLA-4) Ags.[7,9]

Although the primary benefit of using nonhuman primates in biomedical research is the similarity of their immune system to the human immune system, numerous species-specific differences exist that can affect study designs and outcomes.[10–15] For example, circulating neutrophil leukocytes in humans express both low affinity immunoglobulin Fcγ receptors (FcγR II and III) CD32 and CD16.[16]

Abbreviations: APC, allophycocyanin; BV, brilliant violet; CR, complement receptor; IR ARD, infrared amino reactive dye; MPO, myeloperoxidase; PFA, paraformaldehyde

Received: 2 November 2017 | Revised: 24 September 2018 | Accepted: 13 October 2018

Neutrophils of several nonhuman primate species including rhesus macaques, cynomolgus macaques, African green monkeys, and baboons do not express CD16 (17, our unpublished data). However, the absence of CD16 on nonhuman primate neutrophils cannot be generalized because sooty mangabeys do express this receptor on their polymorphonuclear neutrophilic granulocyte.[17] Additionally, while circulating neutrophils in rhesus macaques are CD32 positive, the same cells in African green monkeys are CD32 negative (our unpublished data).

Differences between humans and rhesus macaques exist in the expression patterns of CD11c (CR4) and CD64 (high affinity FcγR I; our unpublished data). Disparities between the immunophenotypes of mature neutrophils raise the possibility of disparities between the differentiation phenotypes of neutrophil progenitors between the two species. Thus, defining characteristic immunophenotype profiles of the different neutrophil progenitor populations in rhesus macaques is necessary. Unfortunately, established differentiating markers used for human samples are of limited value for rhesus macaque samples. For example, an Ab recognizing the CD15 Ag in rhesus macaques is not available. The Ab specific for CD33 (clone AC104.3E3) does not cross-react in a large number of animals tested, and the CD49d Ag expression pattern does not allow reliable separation of the CD49d positive and negative populations.

In the current study we sought to establish a flow cytometric protocol with differentiation markers that unequivocally define distinct subsets, and provide a tool to accurately quantitate neutrophil progenitors in the bone marrow of rhesus macaques. We compared our panel of markers between healthy adult human and rhesus samples to determine similarity and species-specific differences.

2 | MATERIALS AND METHODS

2.1 | Human bone marrow and blood samples

We purchased de-identified, freshly obtained human bone marrow and matching blood samples from 18–65 years old healthy individuals from AllCells LLC (Boston, MA) or Lonza Inc. (Mapleton, IL). The donors signed a procedure-specific consent form. Pregnant women were not included in the study.

2.2 | Animals

We used freshly obtained whole blood and bone marrow from 1.5–9 years old healthy Indian rhesus macaques (*Macaca mulatta*). The animals in this study were assigned to various protocols approved by the University of Wisconsin Institutional Animal Care and Use Committee. They were cared for according to the NIH "Guide to the Care and Use of Laboratory Animals."

2.3 | Flow cytometric staining, data acquisition, and analysis

We dispersed the bone marrow cells in RPMI containing 10% FCS, and filtered them through a 100 μm cell strainer. We stained 10^6 cells in 100 μl tissue culture medium or 100 μl EDTA anticoagulated whole blood at room temperature with CD3 Alexa488 (clone SP34-2), HLA-DR FITC (clone L243), CD123 FITC (clone 7G3), CD66a-e PerCP-Vio700 (clone TET2, Miltenyi, Auburn, CA), CD11b PE-Cy7 (clone ICRF44), CD64 brilliant violet (BV) 510 (clone 10.1 BioLegend, San Diego, CA), CD34 BV650 (clone 563, Fisher Scientific, Madison, WI), CD32 BV711 (clone FLI8.26), CD45 BV786 (clone D058-1283), CD23 Alexa700 (clone M-L233), and CD87 allophycocyanin (APC; clone VIM5, Fisher Scientific, Madison, WI). Abs were obtained from BD Biosciences (San Jose, CA) unless indicated otherwise. We used Near Infrared Amino Reactive Dye (IR ARD; Life Technologies, Carlsbad, CA) to label dead cells. Each reagent was titered for optimal performance. After 15 min of incubation, we added 1 ml of 1× BD Pharm Lysing Solution (BD Biosciences, San Jose, CA) for 5 min. After 2 washing steps, we enhanced the CD87 APC signal using APC Faser Kit (Miltenyi, Auburn, CA). We fixed the cells with 125 μl of 2% paraformaldehyde (PFA) for 15 min, pelleted them at 530 rcf for 5 min, and replaced the PFA, with 100 μl of Bulk Permeabilization reagent (Life Technologies, Carlsbad, CA). We stained for the intracellular Ags with anti-lactoferrin PE Ab (clone 4C5, Fisher Scientific, Madison, WI), and anti-myeloperoxidase (MPO) eFluor450 Ab (clone MPO455-8E6, eBioscience, Madison, WI) for 15 min. Following 2 washing steps, we acquired the data on a BD LSR-II flowcytometer (Becton Dickinson, San Jose, CA) using FACSDiva™ 8.0.1. software. We analyzed the data with FlowJo™ 10.2 (Tree Star Inc., Ashland, OR).

2.4 | Cell sorting

We stained 10^7 bone marrow cells with CD3 FITC (clone SP34-2), CD123 FITC (clone 7G3), HLA-DR FITC (clone L243), Near IR ARD live/dead discriminator dye, CD11b PE-Cy7, and CD87 APC in 200 μl of RPMI—10% FCS. Following a 15-min incubation period, we removed the RBCs with Pharm Lysing Solution. We enhanced the CD87 staining with the APC Faser kit. Sorting was performed with a FACSJazz cell sorter (Becton Dickinson, San Jose, CA) under biosafety level-3 conditions. Cell aggregates, dead cells, T cells, basophil granulocytes, macrophages, and B cells were excluded from the sort strategy. We collected between 17,000 and 93,000 cells for nuclear morphology analysis. Cells were spun onto a 7 mm diameter area of a glass microscope slide using 530 rcf for 5 min, then stained with Wright–Giemsa stain (Wescor Aerospray® Hematology Slide Stainer/Cytocentrifuge, model 7150, Logan, UT).

2.5 | Identification of neutrophil maturational stage

Neutrophil maturational stage was based on generally accepted criteria of nuclear shape for veterinary species.[18] Segmented nuclei contained 2 or more lobes connected by nuclear segments that were less than one-half the width of the widest lobe. Band nuclei were S- or U-shaped with parallel sides lacking distinct segmentation; any narrowing of the nucleus had to maintain a width greater than one-half the width of the thickest part of the nucleus. Metamyelocyte nuclei were elongate ovals with an indentation (reniform). Myelocyte nuclei were round or oval without an indentation. Percentages of

each maturational stage and leukocyte type were based on 300 cell differential counts.

2.6 | In vitro stimulation assays

Briefly, 100 μl whole blood or 10^6 freshly processed bone marrow cells were stimulated with 1 μg/ml LPS, PMA, or 1 μM fMLP for 15 min at 37°C in a 5% CO_2 incubator. Following the stimulation, we stained the cells for surface Ags CD3, HLA-DR, CD123, CD66a-e, CD11b, CD64, CD32, CD45, CD34, CD23, CD87, and stimulation-induced lactoferrin and MPO release. We differentiated live cells from dead ones again with the Near IR ARD. After 15 min of staining, we removed the RBCs with 1 ml of 1× BD Pharm Lysing Solution. Following 2 washing steps, the CD87 APC signal was enhanced with the APC Faser Kit. Cells were fixed with 125 μl of 2% PFA for 15 min, pelleted, and permeabilized with 100 μl of Bulk Permeabilization reagent. We removed the permeabilization buffer with 2 washing steps and then acquired the flow cytometric data.

2.7 | Statistical analysis

For statistical analysis, we employed Students' paired *t* test using Microsoft Excel software version 16.16.1 for Macintosh.

3 | RESULTS AND DISCUSSION

Our goal was to establish a flow cytometric method for the quantification of neutrophil progenitor populations in the bone marrow of rhesus macaques. To that end, we had to find immunologic markers that defined separate differentiation stages reproducibly and unequivocally. We designed a multicolor flow cytometry panel selecting the CD11b, CD32, CD64, CD87, lactoferrin, and MPO Ags due to their established timeline in human neutrophil maturation.[4] CD11b mediates complement-coated pathogen uptake and regulates leukocyte adhesion as part of the CD11b/CD18 heterodimer.[19,20] In humans, the absence of CD11b separates myeloblasts and promyelocytes from later neutrophil progenitor populations, as this Ag first appears at the myelocyte stage.[21] The low affinity γ immunoglobulin receptor CD32 appears as early as the myeloblast stage in humans, and its expression increases in the segmented neutrophil stage.[8,22] The high affinity γ immunoglobulin receptor CD64 expression is maintained at a very low level until it is entirely down-regulated at the band stage in humans.[8,22,23] CD87 (urokinase plasminogen activator receptor) has been described as a marker to identify the band and segmented neutrophil populations in human bone marrow.[24] MPO can be detected in the primary azurophilic granules from the promyelocyte phase to the fully matured segmented neutrophils.[7,25–27] Lactoferrin, a multifunctional protein with antimicrobial activity, appears first in the secondary granules at the metamyelocyte stage of human granulopoiesis.[7,28–30]

As the initial step of our analysis, we excluded lymphocytes, basophil and eosinophil granulocytes, stem cells, macrophages, dead cells, and cell aggregates (SFig. 1). Then we used principal component analysis to 2 components to identify those markers that accounted for the most variance within the CD66a-e$^+$CD23$^-$ gate, and thus defined distinct cell subsets robustly (Fig. 1A). CD87 (–0.66), CD32 (–0.59), and CD11b (–0.38) possessed the highest Eigenvalues in the Eigenvector of the first component, which accounted for 70% of the variance. CD11b (0.55) and CD64 (0.48) had the highest Eigenvalues in the Eigenvector of the second component, which accounted for additional 9.4% of the variance. Based on these results, we selected CD11b and CD87 in a bivariate dot plot display to define 4 well-separated populations (designated I through IV; Fig. 1B). These populations covered the principal component analysis dot plots entirely and on mutually exclusive manner (Fig. 1C). The relative frequency of the populations from I through IV were: 10.1 ± 7.6, 13.6 ± 7.3, 21.6 ± 7.5, and 49.4 ± 8.5% of the parent population, respectively ($n = 5$).

Next, we determined the expression patterns of MPO, lactoferrin, CD32, and CD64 in these populations. MPO and lactoferrin were present in all 4 populations. While the MPO content/cell decreased, the intracellular level of lactoferrin increased in the consecutive populations (Table 1). We detected CD64 on the cell surface at the CD11b$^+$CD87$^-$ phase (population II), and cells remained positive for this protein throughout the final stages of granulopoiesis (Fig. 2D–F). Thus, emergence of CD64 coincided with the appearance of CD11b, but preceded CD87 expression. On the other hand, CD32 first appeared in population III (Fig. 1D and E) with increased expression in population IV (Fig. 2C–F, Table 1). To summarize the data above, we can refine the immunophenotype of the 4 populations as follows:

Population I. CD66$^+$CD11b$^-$CD87$^-$MPO$^+$lactoferrin$^+$CD64$^-$CD32$^-$
Population II. CD66$^+$CD11b$^+$CD87$^-$MPO$^+$lactoferrin$^+$CD64$^+$CD32$^-$
Population III. CD66$^+$CD11b$^+$CD87$^+$MPO$^+$lactoferrin$^+$CD64$^+$CD32$^+$
Population IV. CD66$^+$CD11b$^+$CD87^{++}MPO$^+$lactoferrin$^+$CD64$^+$CD32^{++}

Immunophenotype of the neutrophil leukocytes in the peripheral blood shared the characteristics of population IV (Fig. 2F and G, Table 1).

In humans, CD11b can be detected at the myelocyte stage first,[21] and the appearance of CD87 on the cell surface indicates the final steps (bands and segmented neutrophils) of maturation.[24] However, the expression pattern of CD11b and CD87 Ags together on neutrophil progenitors has not been published. To validate our staining panel for rhesus macaques, we stained human bone marrow samples. While we found similarities between the two species, we also identified one major difference originating from three different levels of CD11b expression. In human samples, CD87 and CD11b defined five separate sub-populations that we designated, I, II, III, IIIa, and IV (Fig. 2H). The phenotype of these populations can be defined as (Fig. 2I–M):

Population I. CD66$^+$CD11b$^-$CD87$^-$MPO$^+$lactoferrin$^+$CD64$^-$CD32$^-$
Population II. CD66$^+$CD11b$^+$CD87$^-$MPO$^+$lactoferrin$^+$CD64$^{+/-}$CD32$^{+/-}$
Population III. CD66$^+$CD11b^{++}CD87$^-$MPO$^+$lactoferrin$^+$CD64$^{+/-}$CD32$^{+/-}$
Population IIIa. CD66$^+$CD11b$^+$CD87$^+$MPO$^+$lactoferrin$^+$CD64$^-$CD32$^{+/-}$
Population IV. CD66$^+$CD11b^{++}CD87^{++}MPO$^+$lactoferrin$^+$CD64$^{+/-}$CD32^{++}

The relative frequency of the populations from I through IV within the CD66a-e$^+$CD23$^-$ gate were: 4.3 ± 0.7, 4.0 ± 0.5, 1.1 ± 0.9, 30.7 ± 6.3, and 56.1 ± 7.3%, respectively ($n = 5$).

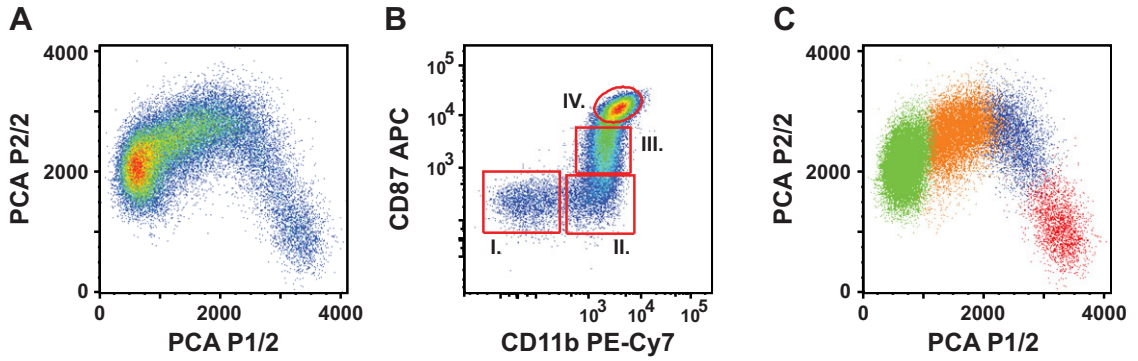

FIGURE 1 **Principal component analysis of neutrophil progenitor immunophenotype markers in the bone marrow of rhesus macaques.** (A) Principal component analysis for 2 components. Plot is based on the expression of 8 (CD10, CD11b, CD32, CD64, CD66, CD87, lactoferrin, and MPO) different parameters. (B) CD11b/CD87-defined populations I–IV. Single, live, CD66a-e positive cells, negative for CD3, CD123, HLA-DR, CD34, and CD23 Ags were gated as shown in Supplementary Fig. 1. (C) Relative location of populations I–IV on the principal component analysis plot. Red, population I; blue, population II; orange, population III; and green, population IV

TABLE 1 The neutrophil progenitor populations defined by the CD11b and CD87 markers display different expression level of the CD64, CD32, lactoferrin, and MPO Ags

	Population	CD64	CD32	Lactoferrin	MPO	CD11b	CD87
Rhesus macaques	I	338 ± 92	95 ± 101	946 ± 267	6320 ± 1916	46 ± 17	327 ± 59
	II	1019 ± 254**	235 ± 156**	2138 ± 742*	4110 ± 946*	1397 ± 670**	333 ± 76
	III	1477 ± 390*	479 ± 176**	4155 ± 1166**	3254 ± 707*	1766 ± 944	1384 ± 633*
	IV	1278 ± 281	1654 ± 529**	5201 ± 1490	3823 ± 1205	2821 ± 1671*	6989 ± 4425*
	Neutrophils in blood	1125 ± 507	2753 ± 1085*	5920 ± 1114	5582 ± 2840	2571 ± 1449	5428 ± 1532
Human samples	I	515 ± 94	181 ± 45	862 ± 134	7478 ± 5236	73 ± 47	333 ± 90
	II	516 ± 109	193 ± 34	1013 ± 158	3972 ± 2510*	1519 ± 573**	586 ± 107**
	III	430 ± 85	345 ± 71	1762 ± 660	2532 ± 1561	9530 ± 4353*	1247 ± 309**
	IIIa	325 ± 43	1107 ± 418*	3142 ± 959*	3076 ± 2182	2754 ± 1215*	1988 ± 426**
	IV	302 ± 53	1484 ± 316**	2330 ± 1250	2247 ± 1370	13039 ± 5215**	4364 ± 2371**
	Neutrophils in blood	307 ± 25	3339 ± 576*	11234 ± 5514	11688 ± 2340*	9986 ± 2404	5774 ± 1756

Numbers are the average of Geometric Mean of Fluorescence Intensity ± SD ($n = 5$), *$P < 0.05$, **$P < 0.005$ difference from the previous population listed in the table

As the phenotype of >97% of the circulating neutrophils resembled the phenotype of population IV (Table 1, Fig. 2B), we proposed that population I represents the most immature, and population IV is the most mature subset. To confirm this hypothesis, we sorted the CD11b/CD87-defined subsets and determined their cellular composition by nuclear morphology-based staging. We found overlap between the morphologically identified stages and the flow cytometry-based immunophenotypic categorization. In rhesus, myelocytes and metamyelocytes represented the majority of population I: 30 ± 15 and 59 ± 8%, respectively with 5 ± 5% presence of each of the band and segmented neutrophils. Population II contained negligible numbers of myelocytes 1±1%, 18±8% metamyelocytes, 44 ± 22% band, and 37 ± 28% segmented neutrophils. Population III consisted of 2 ± 2% of metamyelocytes, 53 ± 23% band, and 44 ± 24% segmented neutrophils, whereas the overwhelming majority 92 ± 6% of population IV was segmented neutrophils with 8 ± 5% of bands (Fig. 3A and C–F). These results indeed support our hypothesis that population I represents cells at the less mature stage and the differentiation pathway leads toward population IV. We quantitated the heterogeneity of the populations classified by their nuclear morphology (Fig. 3B). We found that in rhesus, myelocytes display almost exclusively the population I phenotype (97 ± 4.5%), metamyelocytes are a combination of populations I and II (51.6 ± 32.9 and 49.9 ± 39.4%, respectively), bands are mainly a mix of populations II and III (39.4 ± 3.7 and 51.1 ± 9.0%, respectively), and the segmented neutrophils are a combination of III and IV (22.9 ± 5.5 and 63.8 ± 18%, respectively). A more complex picture emerges in humans (Fig. 3G–M). Most myelocytes display either population I or II phenotype (34.3 ± 7.7 and 43.8 ± 1.8%, respectively). This is primarily due to the earlier expression of CD11b, compared to the differentiation in rhesus macaques. Interestingly, in mice, CD11b and CD32 are expressed on the cell surface throughout the entire granulopoiesis.[31] Although metamyelocytes can be found in populations I, II, and IIIa (Fig. 3L), the majority of them (63.5 ± 3%) display III phenotype (Fig. 3M). Bands may express population IIIa, III, or IV phenotype (20.5 ± 8.8, 23.7 ± 25.4, and 35.7 ± 35%, respectively), showing high variability between different individuals. The majority of segmented neutrophils were found in populations IIIa and IV (24.2 ± 18 and 67.8 ± 8.8%, respectively). The data summarized in Fig. 3 provide evidence that the induction of nuclear segmentation and the changes in these immunophenotypic markers are not strongly connected.

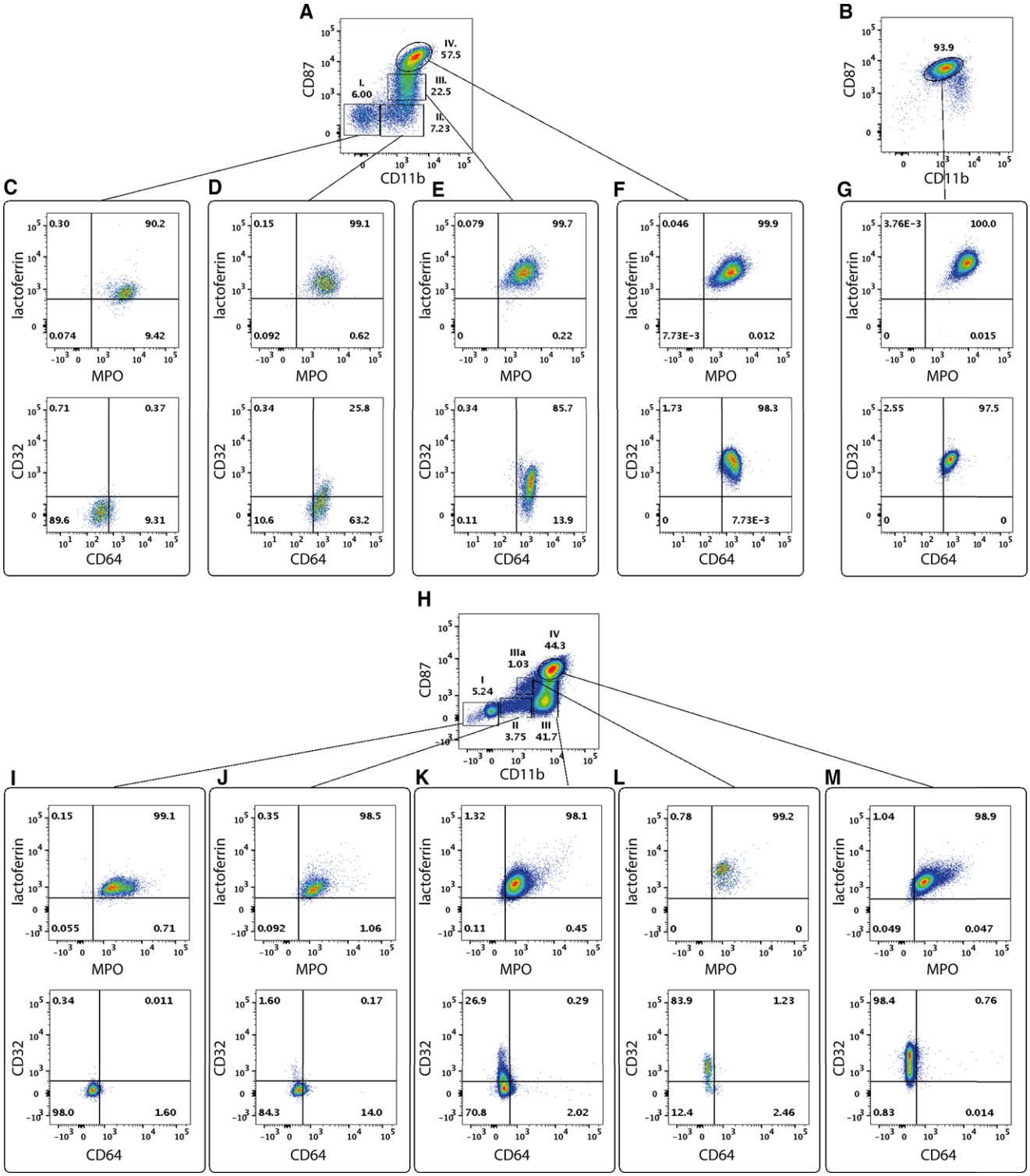

FIGURE 2 **Neutrophil progenitor populations defined by the CD11b and CD87 expression pattern possess distinct immunophenotypes.** (A) Populations I–IV according to their CD11b-CD87 expression pattern in rhesus macaque bone marrow. (B) CD11b/CD87 expression by neutrophil leukocytes in rhesus macaque peripheral blood. (C–F) Lactoferrin, MPO, CD64, and CD32 expressions of populations I, II, III, and IV in rhesus macaque bone marrow. (G) Lactoferrin, MPO, CD64, and CD32 expressions by neutrophil granulocytes in rhesus macaque blood. (H) Populations I–IV according to their CD11b-CD87 expression pattern in human bone marrow. (I–M) Lactoferrin, MPO, CD64, and CD32 expressions of populations I, II, IIIa, III, and IV in human bone marrow

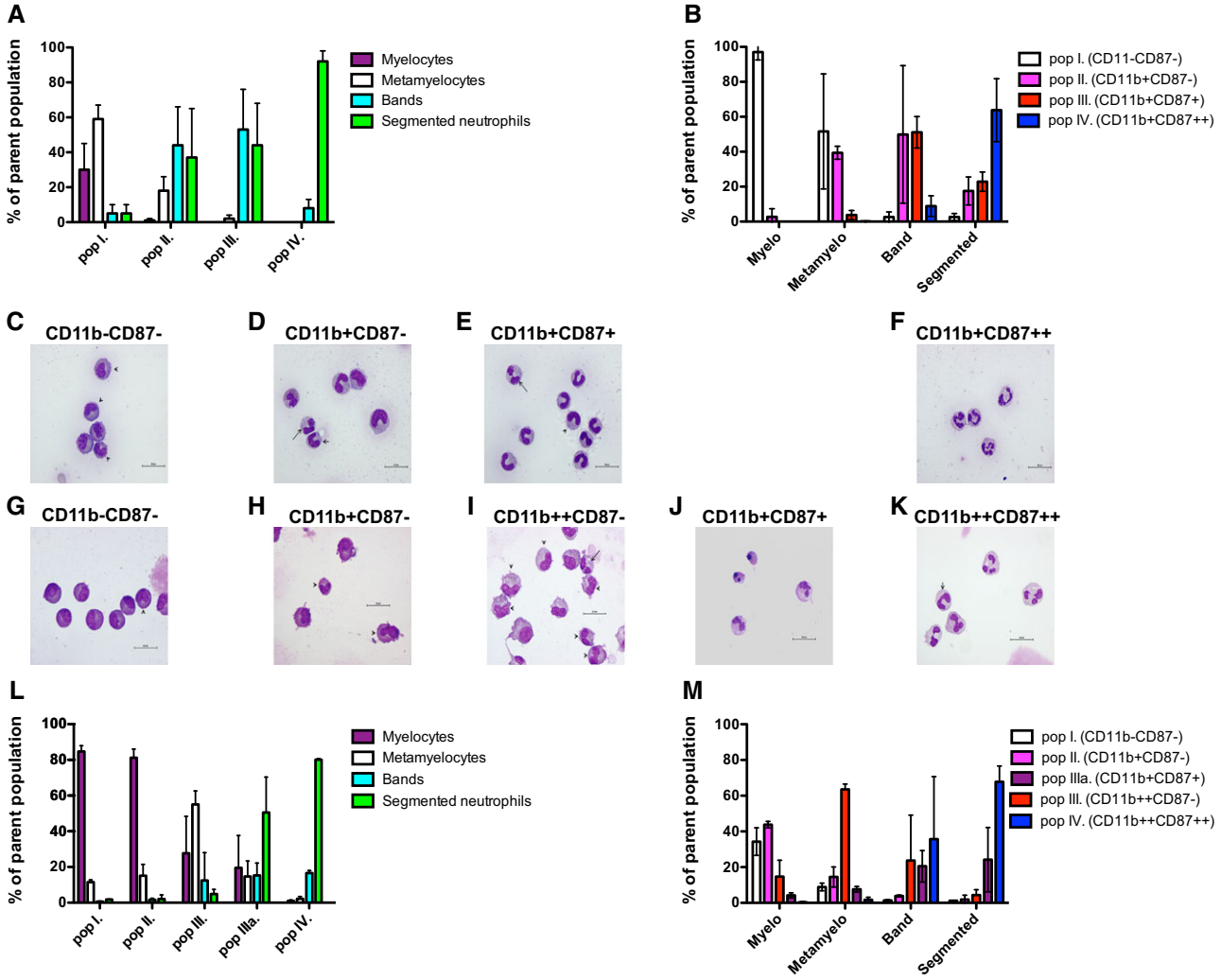

FIGURE 3 Cellular composition of the CD11b/CD87-defined populations. Cells were sorted as detailed in the Materials and Methods section. (A–F) Display data from rhesus macaque samples. (G–M) Data from human samples. (A) Relative frequency of the neutrophil progenitors within the 4 CD11b/CD87 subsets (mean ± SD; $n = 3$). (B) Relative frequency of the CD11b/CD87 subsets within the neutrophil progenitor populations defined by nuclear morphology classification. Representative photomicrographs of subsets described as (C) population I: 3 metamyelocytes and 2 myelocytes; (D) population II: 1 segmented, 1 band, and 3 metamyelocyte neutrophils; (E) population III: 1 segmented, 7 band, and 1 metamyelocyte neutrophils; and (F) population IV: 4 segmented neutrophils in a rhesus macaque sample. Representative photomicrographs of subsets described as (G) population I: 1 metamyelocyte and 7 myelocytes; (H) population II: 2 metamyelocytes and 2 myelocytes; (I) population III: 6 metamyelocytes, 3 myelocytes, 6 metamyelocytes, and 1 segmented neutrophil; (J) population IIIa: 2 segmented neutrophils and 2 pyknotic cells; and (K) population IV: 4 segmented and 1 band neutrophil in a human bone marrow sample. Segmented neutrophils, long arrow; band, medium arrow; and metamyelocytes, short arrow (×1000 magnification). (L) Relative frequency of the neutrophil progenitors within the 5 CD11b/CD87 subsets. (M) Relative frequency of the CD11b/CD87 subsets within the neutrophil progenitor populations defined by nuclear morphology classification

It is important to emphasize here that while CD87 is expressed at the two terminal stages of neutrophil differentiation in rhesus, it is only found on 53.9 ± 3.1% of band, and 83 ± 7.5% ($n = 3$) of segmented neutrophils at detectable levels. (None of the myelocytes and less than 5% of the metamyelocytes [4.3 ± 3.5] are CD87 positive). Therefore, this marker alone cannot be used to quantitate all band and segmented neutrophils in the bone marrow of rhesus macaques.

Next, to assess the functional capabilities of each neutrophil progenitor population subset, we stimulated matching blood and bone marrow samples in vitro with either LPS, fMLP, or PMA. We monitored the level of CD11b expression (Fig. 4A–C), and the release of lactoferrin and MPO to the cell surface (Fig. 4D–F) as indicators of activation.[32,33] Interestingly, while PMA induced significant changes in the phenotype of populations II–IV, neither LPS nor fMLP elicited activation in these populations. We detected LPS-induced CD11b increases only in the blood-derived neutrophil population of rhesus macaques (Fig. 4G and I). In the human samples, however, we measured significant increase of CD11b expression and lactoferrin-positive cell frequency after LPS and PMA treatments in bone marrow populations III and IV, which matched changes in blood samples (Fig. 4H and J). We found no measurable response to LPS and fMLP in populations I, II, and IIIa. These data suggest that while the human neutrophil progenitors complete their entire maturation in the bone marrow, the situation in rhesus macaques could be different.

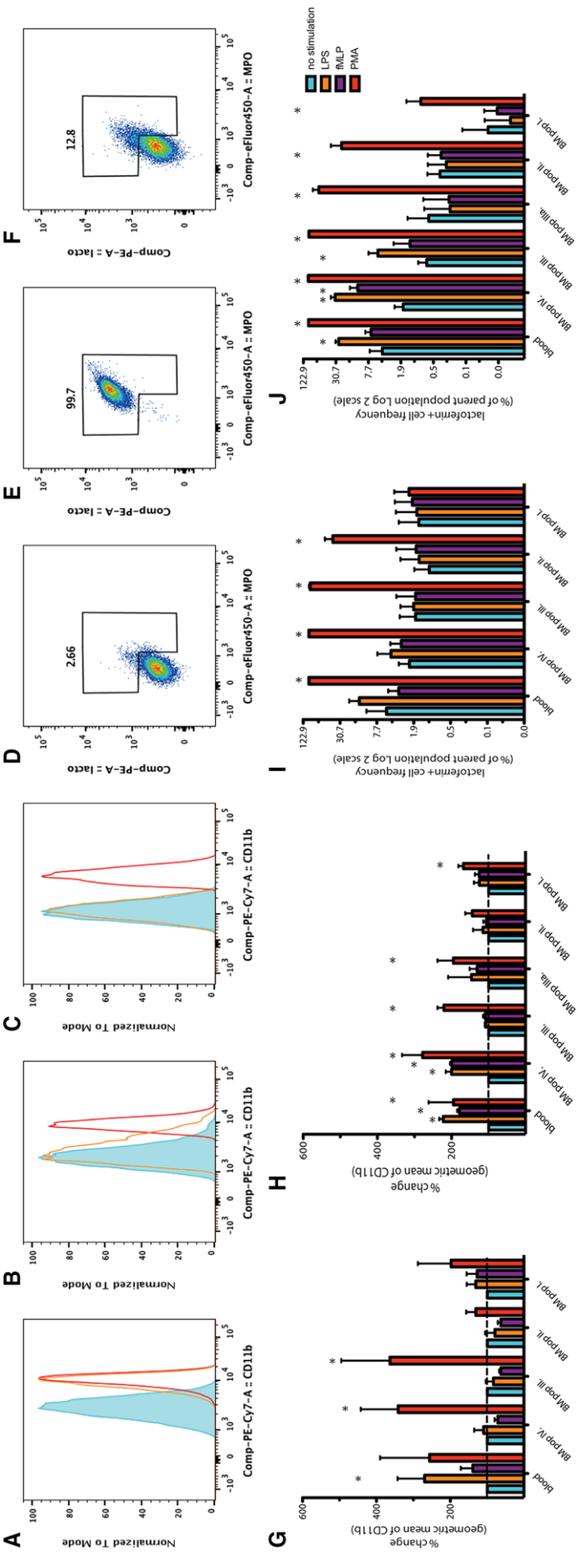

FIGURE 4 **Stimulation induced phenotype changes of neutrophil lineage cells in rhesus macaque or human samples.** (A) CD11b expression by neutrophils in blood; (B) population IV in bone marrow; (C) and population III in the bone marrow of a healthy rhesus macaque. Red histogram, PMA stimulation; yellow histogram, LPS stimulation; blue histogram, unstimulated sample. (D) Surface lactoferrin/MPO in unstimulated; (E) PMA stimulated, or (F) LPS stimulated neutrophils in the blood of a healthy rhesus macaque. (G) Stimulation induced increase of the geometric mean fluorescence of CD11b in rhesus macaque blood and bone marrow ($n = 3$), or (H) in human blood and bone marrow ($n = 3$). (I) Stimulation induced increase of the frequency of lactoferrin/MPO surface positive cells in rhesus macaque blood and bone marrow ($n = 3$), or (J) in human blood and bone marrow ($n = 3$)

Perhaps neutrophils in rhesus macaques reach full maturation at another anatomical site. Several studies have provided evidence for this to occur in mice.[34,35]

Herein we have provided a flow cytometry-based method to characterize four immunophenotypically different subsets of neutrophil progenitors in rhesus macaques. With this protocol, we have introduced a technique that offers improved sensitivity and more dimensionality than the traditional nuclear morphology-based classification. Most importantly this method enables us to monitor the functional aspect of neutrophil maturation. It can be easily combined with applications addressing scientific questions at the genome or transcriptome level. We filled in an important knowledge gap that allows correct data interpretation of studies conducted in rhesus macaque model systems. It will be particularly beneficial for solid organ transplantation research, where extensive surgery induces emergency granulopoiesis, and infectious disease studies, where control of pathogenesis might depend on the homeostasis of neutrophil leukocytes.[36,37]

AUTHORSHIP

K.L.W. was associated with investigation and writing. L.J.V. was associated with investigation. N.L.P. was associated with investigation. J.M.H. was associated with investigation. H.A.S. was associated with data curation. K.R.F. was associated with data curation and writing. E.G.R. was associated with conceptualization, data curation, and writing.

ACKNOWLEDGMENTS

This work was supported by NIH grant #5P51OD011106 to the Wisconsin National Primate Research Center at the University of Wisconsin-Madison. Animals were handled in accordance with the standards of the American Association for the Accreditation of Laboratory Animal Care (AAALAC). We are grateful to Dr. Eileen Maher for editing our manuscript and Ms. Jessica Furlott for her technical assistance.

DISCLOSURES

The authors declare no conflicts of interest.

REFERENCES

1. Nathan C. Neutrophils and immunity: challenges and opportunities. *Nat Rev Immunol*. 2006;6:173–182.
2. Mantovani A, Cassatella MA, Costantini C, Jaillon S. Neutrophils in the activation and regulation of innate and adaptive immunity. *Nat Rev Immunol*. 2011;11:519–531.
3. Lahoz-Beneytez J, Elemans M, Zhang Y, et al. Human neutrophil kinetics: modeling of stable isotope labeling data supports short blood neutrophil half-lives. *Blood*. 2016;127:3431–3438.
4. Pillay J, den Braber I, Vrisekoop N, et al. In vivo labeling with 2H2O reveals a human neutrophil lifespan of 5.4 days. *Blood*. 2010;116:625–627.
5. Kruger P, Saffarzadeh M, Weber AN, et al. Neutrophils: between host defence, immune modulation, and tissue injury. *PLoS Pathog*. 2015;11:e1004651.
6. Slukvin II. Hematopoietic specification from human pluripotent stem cells: current advances and challenges toward de novo generation of hematopoietic stem cells. *Blood*. 2013;122:4035–4046.
7. Mora-Jensen H, Jendholm J, Fossum A, et al. Technical advance: immunophenotypical characterization of human neutrophil differentiation. *J Leukoc Biol*. 2011;90:629–634.
8. Elghetany MT. Surface antigen changes during normal neutrophilic development: a critical review. *Blood Cells Mol Dis*. 2002;28:260–274.
9. Pedersen CC, Borup R, Fischer-Nielsen A, et al. Changes in Gene expression during G-CSF-induced emergency granulopoiesis in humans. *J Immunol*. 2016;197:1989–1999.
10. Bontrop RE, Watkins DI. MHC polymorphism: AIDS susceptibility in non-human primates. *Trends Immunol*. 2005;26:227–233.
11. Carter DL, Shieh TM, Blosser RL, et al. CD56 identifies monocytes and not natural killer cells in rhesus macaque. *Cytometry*. 1999;37:41–50.
12. Dykhuizen M, Ceman J, Mitchen J, et al. Importance of the CD3 marker for evaluating changes in rhesus macaque CD4/CD8 T-cell ratios. *Cytometry*. 2000;40:69–75.
13. LaBonte ML, Choi EI, Letvin NL. Molecular determinants regulating the pairing of NKG2 molecules with CD94 for cell surface heterodimer expression. *J Immunol*. 2004;172:6902–6912.
14. Reeves RK, Gillis J, Wong FE, et al. CD16- natural killer cells: enrichment in mucosal and secondary lymphoid tissues and altered function during chronic SIV infection. *Blood*. 2010;115:4439–4446.
15. Sugimoto C, Hasegawa A, Saito Y, et al. Differentiation kinetics of blood monocytes and dendritic cells in macaques: insights to understanding human myeloid cell development. *J Immunol*. 2015;195:1774–1781.
16. Bruhns P. Properties of mouse and human IgG receptors and their contribution to disease models. *Blood*. 2012;119:5640–5649.
17. Rogers KA, Scinicariello F, Attanasio R. IgG Fc receptor III homologues in nonhuman primate species: genetic characterization and ligand interactions. *J Immunol*. 2006;177:3848–3856.
18. Radin MJ, Wellman ML. Granulopoiesis. In: Weiss DJ, Wardrop KJ, eds. *Schalm's Veterinary Hematology*. 6th ed. Ames, IA: Wiley Blackwell; 2010:43–49.
19. Jones DH, Anderson DC, Burr BL, et al. Quantitation of intracellular Mac-1 (CD11b/CD18) pools in human neutrophils. *J Leukoc Biol*. 1988;44:535–544.
20. Beller DI, Springer TA, Schreiber RD. Anti-Mac-1 selectively inhibits the mouse and human type three complement receptor. *J Exp Med*. 1982;156:1000–1009.
21. Terstappen LW, Safford M, Loken MR. Flow cytometric analysis of human bone marrow. III. Neutrophil maturation. *Leukemia*. 1990;4:657–663.
22. Fleit HB, Wright SD, Durie CJ, Valinsky JE, Unkeless JC. Ontogeny of Fc receptors and complement receptor (CR3) during human myeloid differentiation. *J Clin Invest*. 1984;73:516–525.
23. Nimmerjahn F, Ravetch JV. Fcgamma receptors: old friends and new family members. *Immunity*. 2006;24:19–28.
24. Elghetany MT, Patel J, Martinez J, Schwab H. CD87 as a marker for terminal granulocytic maturation: assessment of its expression during granulopoiesis. *Cytometry B Clin Cytom*. 2003;51:9–13.
25. Gadd SJ, Majdic O, Kasinrerk W, et al. M5, a phosphoinositol-linked human myelomonocytic activation-associated antigen. *Clin Exp Immunol*. 1990;80:252–256.
26. Bainton DF. Selective abnormalities of azurophil and specific granules of human neutrophilic leukocytes. *Fed Proc*. 1981;40:1443–1450.

27. Nauseef WM, Olsson I, Arnljots K. Biosynthesis and processing of myeloperoxidase–a marker for myeloid cell differentiation. *Eur J Haematol*. 1988;40:97–110.
28. Borregaard N, Sørensen OE, Theilgaard-Mönch K. Neutrophil granules: a library of innate immunity proteins. *Trends Immunol*. 2007;28:340–345.
29. Berliner N, Hsing A, Graubert T, et al. Granulocyte colony-stimulating factor induction of normal human bone marrow progenitors results in neutrophil-specific gene expression. *Blood*. 1995;85:799–803.
30. Bartels M, Govers AM, Fleskens V, et al. Acetylation of C/EBPε is a prerequisite for terminal neutrophil differentiation. *Blood*. 2015;125:1782–1792.
31. Evrard M, Kwok IWH, Chong SZ, et al. Developmental analysis of bone marrow neutrophils reveals populations specialized in expansion, trafficking, and effector functions. *Immunity*. 2018;48:364–379.
32. Soler-Rodriguez AM, Zhang H, Lichenstein HS, et al. Neutrophil activation by bacterial lipoprotein versus lipopolysaccharide: differential requirements for serum and CD14. *J Immunol*. 2000;164:2674–2683.
33. Swain SD, Jutila KL, Quinn MT. Cell-surface lactoferrin as a marker for degranulation of specific granules in bovine neutrophils. *Am J Vet Res*. 2000;61:29–37.
34. Deniset JF, Surewaard BG, Lee WY, Kubes P. Splenic Ly6G^{high} mature and Ly6G^{int} immature neutrophils contribute to eradication of *S. pneumonie*. *J Exp Med*. 2017;214:1333–1350.
35. Chorny A, Casas-Recasens S, Sintes J, et al. The soluble pattern recognition receptor PTX3 links humoral innate and adaptive immune responses by helping marginal zone B cells. *J Exp Med*. 2016;213:2167–2185.
36. Ball ED, McDermott J, Griffin JD, Davey FR, Davis R, Bloomfield CD. Expression of the three myeloid cell-associated immunoglobulin G Fc receptors defined by murine monoclonal antibodies on normal bone marrow and acute leukemia cells. *Blood*. 1989;73:1951–1956.
37. Elbim C, Monceaux V, Mueller YM, et al. Early divergence in neutrophil apoptosis between pathogenic and nonpathogenic simian immunodeficiency virus infections of nonhuman primates. *J Immunol*. 2008;181:8613–8623.

SUPPORTING INFORMATION

Additional information may be found online in the Supporting Information section at the end of the article.

How to cite this article: Weisgrau KL, Vosler LJ, Pomplun NL. Neutrophil progenitor populations of rhesus macaques. *J Leukoc Biol*. 2019;105:113–121. https://doi.org/10.1002/JLB.1TA1117-431RR